

Simulating Redshift-Space Distortions for Galaxy Pairs with Wide Angular Separation

Alvise Raccanelli^{1*}, Lado Samushia^{1,2}, Will J. Percival¹

¹*Institute of Cosmology & Gravitation, University of Portsmouth, Portsmouth, PO1 3FX, UK*

²*National Abastumani Astrophysical Observatory, Ilia State University, 2A Kazbegi Ave, GE-0160 Tbilisi, Georgia*

10 June 2010

ABSTRACT

The analysis of Redshift-Space Distortions (RSD) within galaxy surveys provides constraints on the amplitude of peculiar velocities induced by structure growth, thereby allowing tests of General Relativity on extremely large scales. The next generation of galaxy redshift surveys, such as the Baryon Oscillation Spectroscopic Survey (BOSS), and the Euclid experiment will survey galaxies out to $z = 2$, over $10,000\text{--}20,000 \text{ deg}^2$. In such surveys, galaxy pairs with large comoving separation will preferentially have a wide angular separation. In standard plane-parallel theory the displacements of galaxy positions due to RSD are assumed to be parallel for all galaxies, but this assumption will break down for wide-angle pairs. Szapudi (2004) and Papai & Szapudi (2008) provided a methodology, based on tripolar spherical harmonics expansion, for computing the redshift-space correlation function for all angular galaxy pair separations. In this paper we introduce a new procedure for analysing wide-angle effects in numerical simulations. We are able to separate, demonstrate, and fit each of the effects described by the wide-angle RSD theory. Our analysis highlights some of the nuances of dealing with wide-angle pairs, and shows that the effects are not negligible even for relatively small angles. This analysis will help to ensure the full exploitation of future surveys for RSD measurements, which are currently confined to pair separations less than $\sim 80 h^{-1} \text{ Mpc}$ out to $z \simeq 0.5$.

Key words: cosmological parameters — large scale structure of Universe — cosmology : observations — methods : analytical

1 INTRODUCTION

Many different mechanisms have been suggested to explain the observed late-time acceleration of the expansion of the Universe (Riess et al. 1998; Perlmutter et al. 1999).¹ Differentiating between these options is one of the main challenges facing cosmologists today. We can try to build up the evidence for different mechanisms by examining the evolution of the Universe in two key ways: measuring the background geometry and measuring structure formation within it.

The geometrical evolution of the Universe can most easily be measured using two primary techniques: we can use supernovae as standard candles or galaxy clustering as a standard ruler to make precise measurement of cosmological expansion. Although supernovae were first to confirm the accelerated expansion of the Universe at high statistical significance (Riess et al. 1998; Perlmutter et al. 1999) following analyses of early galaxy surveys

(Efstathiou et al. 1990), supernovae surveys are now limited by systematic rather than statistical errors (Kessler 2009). The possibility of using galaxy clustering to provide a standard ruler has become increasingly important since the baryon acoustic peak was detected (Percival et al. 2001; Cole et al. 2005; Eisenstein et al. 2005) in galaxy power spectra measured from the 2dF Galaxy Redshift Survey (2dFGRS; Colless et al. 2003) and the Sloan Digital Sky Survey (SDSS; York et al. 2000). Using only the Baryon Acoustic Oscillation (BAO) component of the galaxy clustering signal makes constraints robust to non-linear effects, and has already been exploited to produce interesting constraints on cosmological models (Percival et al. 2007a,b; Gaztanaga et al. 2008; Sanchez et al. 2009; Percival et al. 2010).

Galaxy surveys provide complementary information about the build-up of large-scale structure through Redshift Space Distortions (RSD). These arise because we do not observe true galaxy positions, but instead infer distances from measured redshifts. Coherent comoving galaxy velocities due to the growth of structure therefore lead to measurable anisotropic clustering (Kaiser 1987; Hamilton 1998). RSD have been measured from the 2dFGRS and SDSS using techniques based on both correlation

* e-mail: alvise.raccanelli@port.ac.uk (AR)

¹ For a recent review of dark energy see, e.g., (Frieman, Turner & Huterer 2008) and references therein.

functions and power-spectra (Peacock et al. 2001; Hawkins et al. 2003; Percival et al. 2004; Pope et al. 2004; Zehavi et al. 2005; Okumura et al. 2008; Cabre & Gaztanaga 2009), and have recently been detected at higher redshift (Guzzo et al. 2009; Blake et al. 2010).

In fact, for fundamental reasons, RSD are independent of galaxy bias: galaxies act as test particles in the matter flow, so their motion is independent of galaxy properties. We can therefore measure the matter velocity field at the locations of the galaxies and, provided that galaxy positions are representative within the velocity field, this gives an unbiased measurement of $f\sigma_8(\text{mass})$ where $f \equiv d \ln D / d \ln a$, the logarithmic derivative of the linear growth rate, $D(z)$, with respect to the scale factor a , and $\sigma_8(\text{mass})$ quantifies the amplitude of fluctuations in the matter density field.

Many techniques have been proposed for measuring RSD, including using multipoles of the correlation function (Hamilton 1992), or the power spectrum (Percival & White 2009), based on the plane-parallel approximation for RSD (Kaiser 1987). The geometry of the system can be easily incorporated into an analysis of the correlation function as the separation of each pair can be split into radial and angular components. It is more difficult to perform such a decomposition when measuring the power spectrum, although various techniques have been suggested, decomposing the density field into a basis of spherical harmonics and radial functions (e.g. Fisher et al. 1994; Heavens & Taylor 1995). As well as allowing for the geometry to a survey and RSD within it, we need to allow for two effects:

(i) RSD are degenerate with the angular anisotropy of power spectrum caused by the Alcock-Palczinski effect, so measurements of growth and geometry from the same survey will be correlated, and it is sensible to undertake a combined analysis (Ballinger et al. 1996; Simpson & Peacock 2009).

(ii) as noted by Hamilton (1998), the full RSD operator has extra terms compared to the plane-parallel one and results in a redshift-space power spectrum which is not diagonal in \mathbf{k} . These extra terms are important for galaxy pairs separated by wide angles and need to be included in any analysis that uses wide-angle data (Szalay et al. 1998; Szapudi 2004; Papai & Szapudi 2008).

In this paper we concentrate on the second of these effects. Szapudi (2004) and Papai & Szapudi (2008) proposed a method of computing the redshift-space correlation function which does not assume a plane-parallel approximation and is applicable to arbitrarily large angles. In their treatment the redshift-space correlation function depends not only on the redshift-space pair separation x and cosine of the angle of the pair with respect to the line-of-sight μ , but also on the separation angle between two galaxies in a pair θ , which does not have to be small. They were able to express the redshift-space correlation function explicitly through a real-space correlation function and cosmological parameters. Given the precision that future surveys will achieve and the fact that they will cover large fractions of the sky, these effects will need to be corrected.

The wide-angle effects can be subdivided in “purely wide-angle” and “mode-coupling” terms: “purely wide-angle” effects correct plane-parallel predictions accounting for the fact that the separation angle is non-zero, “mode-coupling” terms in addition account for the fact that galaxy pairs coherently moved from the high-density to low-density regions. These latter terms vanish if the initial real-space distribution of galaxies is uniform in distance, and both terms vanish in the plane-parallel limit due to the symmetry of the system. Both terms are of the same order and mode-coupling

tends to smooth out features in the power spectrum such as the Baryon Acoustic Oscillations (BAO).

Given the importance and, particularly, the quality of RSD constraints expected from forthcoming surveys such as the Baryon Oscillation Spectroscopic Survey (BOSS; Schlegel et al. 2009a), surveys resulting from proposals for wide-field multi-object spectrographs on 4m telescopes such as BigBOSS (Schlegel et al. 2009b) and satellite missions such as Euclid (Laureijs et al. 2009), it is timely to revisit this problem, and to test wide-angle RSD theory. In this paper we use numerical simulations to extensively test the dependence of RSD constraints on the angular separation of galaxy pairs.

This paper is organised as follows: in Sec. 2 we briefly review the theory of wide-angle RSD; in Sec. 3 we describe a time-efficient method of getting a low-noise measurement of wide-angle correlation function from a mock HV catalog; in Sec. 4 we present our results and discuss all the steps necessary to match measured correlation function with theoretical predictions; in Sec. 5 we conclude and discuss how the results will affect real survey measurements.

2 WIDE-ANGLE REDSHIFT-SPACE DISTORTIONS

Galaxy positions are measured in a redshift-space, and differ from the real-space positions because of the contributions from peculiar velocities,

$$\mathbf{s}(\mathbf{r}) = \mathbf{r} - v_r(\mathbf{r})\hat{\mathbf{r}}, \quad (1)$$

where \mathbf{s} is the redshift space position, \mathbf{r} is the real space position and v_r the radial component of peculiar velocity.

Since the total number of galaxies in real and redshift spaces is the same, the number $N^s(\mathbf{s})d^3s$ of galaxies observed in a volume element d^3s of redshift space is related to the real space number density $N^r(\mathbf{r})$ by:

$$N^s(\mathbf{s})d^3s = N^r(\mathbf{r})d^3r. \quad (2)$$

The observed redshift space galaxy overdensity δ^s at position \mathbf{s} can be related to the redshift-space selection function \bar{N}^s ,

$$\delta^s(\mathbf{s}) = \frac{N^s(\mathbf{s}) - \bar{N}^s(\mathbf{s})}{\bar{N}^s(\mathbf{s})}. \quad (3)$$

In contrast, an unbiased estimate of the true galaxy overdensity δ^r at position \mathbf{r} is given by:

$$\delta^r(\mathbf{r}) = \frac{N^r(\mathbf{r}) - \bar{N}^r(\mathbf{r})}{\bar{N}^r(\mathbf{r})}, \quad (4)$$

where $\bar{N}^r(\mathbf{r})$ is the expected galaxy distribution in real-space – the expected number density of unclustered galaxies at position \mathbf{r} given the selection criteria of the survey.

We distinguish here between the measured redshift-space selection function $\bar{N}^s(\mathbf{s})$ and the true selection function $\bar{N}^r(\mathbf{r})$ even though the two are the same at linear order. We now assume that the expected density is a function of the radial component of the position only, which we denote s in redshift-space and r in real-space. Thus the relation between the observed redshift space overdensity $\delta^s(\mathbf{s})$ and the true overdensity $\delta^r(\mathbf{r})$ is:

$$\bar{N}^s(s)[1 + \delta^s(\mathbf{s})]s^2 ds = \bar{N}^r(r)[1 + \delta^r(\mathbf{r})]r^2 dr. \quad (5)$$

Using Eq. (2) we obtain:

$$1 + \delta^s(\mathbf{s}) = [1 + \delta^r(\mathbf{r})] \left(1 + \frac{\partial v}{\partial r}\right)^{-1} \left(1 + \frac{v}{r}\right)^{-2} \frac{\bar{N}(r)}{N(r + v\hat{r})}, \quad (6)$$

which gives, to linear order:

$$\delta^s(\mathbf{r}) = \delta^r(\mathbf{r}) - \left(\frac{\partial v}{\partial r} + \frac{\alpha(\mathbf{r})v}{r}\right), \quad (7)$$

where

$$\alpha(\mathbf{r}) = \frac{\partial \ln r^2 \bar{N}^s(\mathbf{r})}{\partial \ln r}. \quad (8)$$

Usually the $(1 + \frac{v}{r})^2$ term in the Jacobian is omitted because, in the linear regime, it gives rise to a $2v/r$ term, that would tend to zero at large distances. However, Papai & Szapudi (2008) have argued that, for wide angles, the v/r term is of the same order as the $\partial_r v$ term.

Using the exact Jacobian, and following Papai & Szapudi (2008), we can express the linear overdensity as:

$$\delta^s(r) = \int \frac{d^3 k}{(2\pi)^3} e^{ik_j r_j} \left[1 + f(\hat{r}_j \hat{k}_j)^2 - i\alpha f \frac{\hat{r}_j \hat{k}_j}{rk}\right] \delta(k), \quad (9)$$

so the correlation function is:

$$\langle \delta^s(\mathbf{r}_1) \delta^{s*}(\mathbf{r}_2) \rangle = \int \frac{d^3 k}{(2\pi)^3} P(k) e^{ik(r_1 - r_2)} \left[1 + \frac{f}{3} + \frac{2f}{3} L_2(\hat{r}_1 \hat{k}) - \frac{i\alpha f}{r_1 k} L_1(\hat{r}_1 \hat{k})\right] \left[1 + \frac{f}{3} + \frac{2f}{3} L_2(\hat{r}_2 \hat{k}) + \frac{i\alpha f}{r_2 k} L_1(\hat{r}_2 \hat{k})\right], \quad (10)$$

where L_ℓ are the Legendre polynomials of order ℓ and $P(k)$ is the real-space matter power spectrum. The third terms in the brackets are the ones responsible for the wide-angle effects, while the fourth terms are the ones responsible for the mode-coupling. Note that the r_1 and r_2 terms in the denominator depend on the angular separation of the galaxies. Setting ϕ_1 as the angle between the vector to the first galaxy in a pair \mathbf{r}_1 , \mathbf{x} to be the vector connecting galaxies in a pair, and ϕ_2 to be the angle between vector to the second galaxy in a pair \mathbf{r}_2 and \mathbf{x} , we can use the sine rule (see Fig. 1) to express r_1 and r_2 as

$$r_1 = \frac{\sin(\phi_2)}{\sin(\phi_2 - \phi_1)} x, \quad (11)$$

$$r_2 = \frac{\sin(\phi_1)}{\sin(\phi_2 - \phi_1)} x. \quad (12)$$

Tripolar spherical harmonics are the most natural basis for the expansion of a function that depends on three directions (Varshalovich et al. 1988) so, as suggested in Szapudi (2004) and Papai & Szapudi (2008), we expand Eq. (10) using a subset of them that are proportional to the zero angular momentum:

$$S_{\ell_1 \ell_2 \ell}(\hat{r}_1, \hat{r}_2, \hat{x}) = \sum_{m_1, m_2, m} \begin{pmatrix} \ell_1 & \ell_2 & \ell \\ m_1 & m_2 & m \end{pmatrix} C_{\ell_1 m_1}(\hat{r}_1) C_{\ell_2 m_2}(\hat{r}_2) C_{\ell m}(\hat{x}), \quad (13)$$

where $C_{\ell m}$ are normalized spherical functions, multiplied by the $3j$ Wigner symbol. The redshift space correlation function is then written as:

$$\xi^s(\hat{r}_1, \hat{r}_2, \hat{x}) = \sum_{\ell_1, \ell_2, \ell} B^{\ell_1 \ell_2 \ell}(x, \phi_1, \phi_2) S_{\ell_1 \ell_2 \ell}(\hat{r}_1, \hat{r}_2, \hat{x}), \quad (14)$$

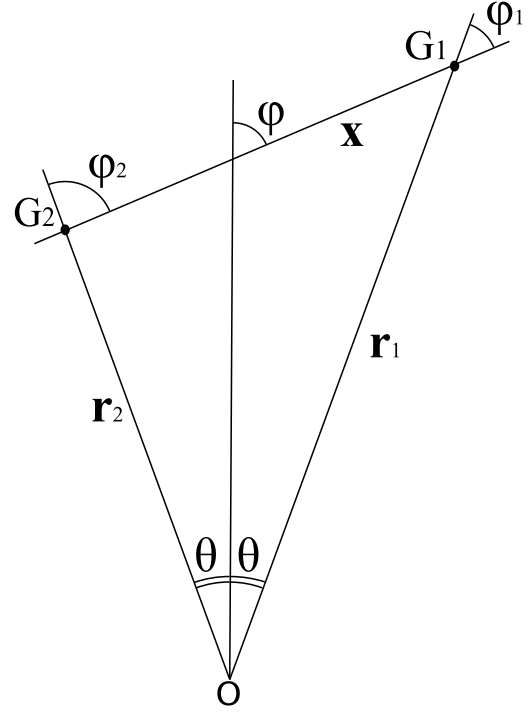


Figure 1. The coordinate system adopted for the triangle formed by the observer O , and galaxies G_1 and G_2 .

where $B^{\ell_1 \ell_2 \ell}(x, \phi_1, \phi_2)$ are a series of coefficients that depend on f , $g_i(\phi_i)$ and $\xi_\ell^r(x)$, and they can be divided into wide-angle components (given in Szalay et al. 1998 & Szapudi 2004) that do not depend on the third term in Eq. (9), and mode-coupling components (given in Papai & Szapudi 2008); the plane-parallel approximation emerges as a limit when $\hat{r}_1 = \hat{r}_2$.

As described in Hamilton & Culhane (1996), for any pair of galaxies we can fully analyse the problem within a plane formed by the two galaxies and the observer; the effect of redshift-space distortions only depends on the geometry within this plane. In the coordinate system described above, the vectors connecting the observer with the galaxies are \mathbf{r}_1 and \mathbf{r}_2 , and the separation vector between the galaxies is \mathbf{x} ; ϕ_i are the angles between \mathbf{r}_i and \mathbf{x} . In the plane parallel approximation $\phi_1 = \phi_2$. This description of the triangle is shown in Fig. 1.

At this point we still have the freedom to choose a line-of-sight to the galaxy pair: we follow the standard approach and choose the line of sight as a direction bisecting the angle formed by the two galaxies, which we assume is given by 2θ . The angle between the angle bisector and \mathbf{x} is denoted ϕ , and we define $\mu \equiv \cos(\phi)$. We therefore have that $\phi = \frac{1}{2}(\phi_1 + \phi_2)$, and $\theta = \frac{1}{2}(\phi_2 - \phi_1)$. This is shown in Fig. 1.

With this choice of coordinate system the redshift-space correlation function can be expanded as:

$$\begin{aligned} \xi^s(x, \theta, \phi) &= \sum_{ab} c_{ab}(x) L_a(\cos(\theta)) L_b(\cos(\phi)), \quad (15) \\ &= \sum_{n_1, n_2} a_{n_1 n_2} \cos(n_1 \phi_1) \cos(n_2 \phi_2) \\ &\quad + b_{n_1 n_2} \sin(n_1 \phi_1) \sin(n_2 \phi_2), \quad (16) \end{aligned}$$

with coefficients given in Papai & Szapudi (2008). Eq. (15) reduces to the plane-parallel result (Hamilton 1992) in the limit of $\theta \rightarrow 0$.

3 MEASURING WIDE-ANGLE CORRELATION FUNCTIONS

A standard method for analysing a N-body simulation to test wide-angle redshift-space distortions would be to:

- (i) locate an observer within the output,
- (ii) translate all galaxies from real into redshift-space based on this observer,
- (iii) sample from these galaxies based on desired radial distribution,
- (iv) split pairs into bins in ϕ , θ , x and counts pairs,
- (v) estimate the correlation function.

This approach mimics that of an actual survey analysis, creating a mock galaxy catalogue. However, if we want to measure the effect of redshift-space distortions for galaxy pairs with a particular angular separation, the method is not optimal as only a small fraction of the galaxy pairs analysed will have this angular separation. In addition, we have to perform the full procedure for every radial galaxy distribution that we wish to analyse, and this distribution will limit the pair-density that can be selected from the simulation. In order to rapidly increase the signal-to-noise, we adopt a different procedure, allowing the origin to move so that each galaxy pair can be analysed as if it was observed with the required angular separation. This procedure can be summarised as follows:

- (i) decide on the value of θ for which we wish to analyse pairs,
- (ii) take each galaxy pair from the simulation with real-space separation $< R_{\max} h^{-1}$ Mpc,
- (iii) for each pair randomly choose $\mu \in [-\cos(\theta), \cos(\theta)]$,
- (iv) choose the location of the origin giving this μ and θ ,
- (v) move galaxies according to their expected redshift-space distortion,
- (vi) weight the pair by a function of μ , x to match desired distribution,
- (vii) split pairs into bins in ϕ , x and counts pairs,
- (viii) estimate the correlation function.

The added complexity of including redshift-space distortions on a pair-by-pair basis is outweighed by the ability to obtain more pairs at the desired angular separation. Note that μ in step (iii) is constrained and cannot have any value within $[-1, 1]$ because $|\phi| > |\theta|$ results in geometrically impossible triangles (see, Fig. 1). The distributions of triangles in μ and x for a galaxy distribution with a power law selection in r can be calculated analytically, as we now demonstrate.

3.1 Real-space distribution of μ , x

The redshift-space correlation function in Eq. (15) depends on the selection function $\alpha(\mathbf{r}) \equiv 2 + \partial \ln[n(\mathbf{r})]/\partial r$, where $n(\mathbf{r})$ is the number density of galaxies in real space and \mathbf{r} is the position of the galaxy from the observer as in Section 2. If the galaxy distribution is uniform ($\alpha(\mathbf{r}) = 2$, $n(\mathbf{r}) = n$, both independent of \mathbf{r}), then the probability of finding a galaxy in some region is proportional to the volume of that region. Therefore if we randomly pick a galaxy in the catalog, there will be on average $n x^2 dx d\mu$ galaxies in a small volume element $dx d\mu$ which is distance $x \pm dx$ away from that galaxy within an angular slice $\mu \pm d\mu$. In the plane-parallel approximation, where all galaxies are assumed to lie along the same direction from the observer, the distribution of galaxy pairs will scale as

$$dN_{\text{pp}}^{\text{pair}}(x, \mu) \propto x^2 dx d\mu, \quad (17)$$

where $dN_{\text{p}}^{\text{pair}} p(x, \mu)$ is the number of pairs with separation $x \pm dx$ and cosine of the angle with the line of sight in the $\mu \pm d\mu$ interval. If we pick galaxy pairs separated by a fixed opening angle from the uniform spatial distribution of galaxies (step (i) in the procedure described above), for a large enough angle the distribution of pairs will not follow Eq. (17). For galaxy pairs with a fixed half-angle θ (see, Fig. 1), the likelihood of finding one galaxy at position \mathbf{r}_1 and another at \mathbf{r}_2 is $P(r_1) \propto r_1^2 dr_1$, $P(r_2) \propto r_2^2 dr_2$. Since the two likelihoods are independent, the joint probability of finding that pair of galaxies is:

$$dN_{\theta}^{\text{pair}}(r_1, r_2) \propto r_1^2 r_2^2 dr_1 dr_2. \quad (18)$$

Using Eqs. (11) and (12) we can rewrite Eq. (18) in terms of ϕ and x as:

$$dN_{\theta}^{\text{pair}}(x, \mu) \propto x^5 \sin(\phi + \theta)^2 \sin(\phi - \theta)^2 dx d\phi. \quad (19)$$

After completing steps (ii) and (iii) in the previous subsection, we will have a distribution of galaxy pairs that is uniform in $d\mu = \sin(\phi) d\phi$ and scales as $x^2 dx$ with separation. This distribution of galaxy pairs does not correspond to $\alpha = 2$. If we want to compare our data with the correlation function computed from Eq. (15) for $\alpha = 2$, we have to weight our galaxy pairs (step (iv) in the previous subsection) by an additional factor of $x^3 \sin(\phi - \theta)^2 \sin(\phi + \theta)^2$ to get a distribution given by Eq. (19).

This procedure can be applied to the case of arbitrary α . If, for example, the galaxy number density scales as a power-law $n(\mathbf{r}) = r^{-N}$, then $\alpha = 2 - N$, and the distribution of galaxy pairs with a fixed opening half-angle drawn from this distribution will be:

$$dN_{\theta}^{\text{pair}}(x, \mu) \propto x^{2\alpha+1} \sin(\phi + \theta)^{\alpha} \sin(\phi - \theta)^{\alpha} dx d\phi. \quad (20)$$

We therefore weight all pairs recovered from the simulation with a weight given by:

$$W(x, \mu) = \frac{x^{2\alpha-1} \sin(\phi_r + \theta)^{\alpha} \sin(\phi_r - \theta)^{\alpha}}{x_s^{2\alpha-1} \sin(\phi_s + \theta)^{\alpha} \sin(\phi_s - \theta)^{\alpha}}, \quad (21)$$

where x_s is the separation of the galaxies in redshift-space, ϕ_r is the real-space value of ϕ for the chosen galaxy pair and ϕ_s is the redshift-space value. We divide the real-space distribution by the redshift-space equivalent in order to normalise the weights to give no net change in the expected pair distribution.

3.2 Redshift-space distribution of μ , x

When transformed into redshift space, the real-space galaxy distribution is ‘‘washed out’’ by the random component of galaxy velocities, so we need to convolve with the random velocity distribution. This would normally not be a problem as we would estimate the galaxy distribution directly in redshift-space. However, using the above procedure we have set the real-space distribution of galaxies, so we need to take care when modelling the redshift-space distribution. To correct for this effect, we first estimate the velocity dispersion σ_v from the catalog, assuming that the random velocities are drawn from a Gaussian distribution. We then convolve the initial distribution in real space with this Gaussian. For example, for $n(\mathbf{r}) \propto r^{-N}$, the probability of finding a galaxy at distance r away from the observer is $P(r) \propto r^{2-N} = r^{\alpha}$. In the unclustered

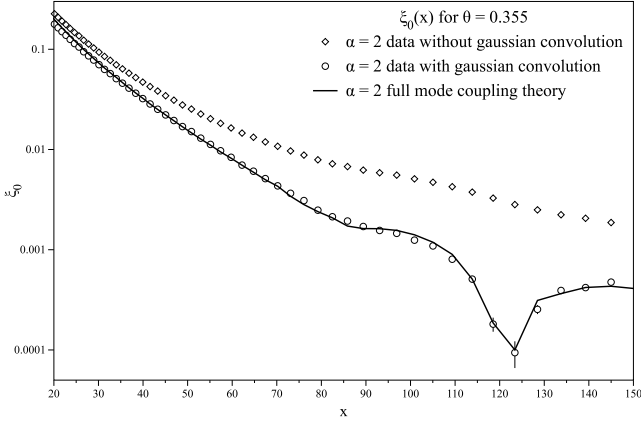


Figure 2. The monopole correlation function calculated from the HV mock catalogues designed to mimic a galaxy distribution with $\theta = 0.355$, and $\alpha = 2$. Open circles (with 1σ errors) were calculated using the redshift-space model for the galaxy distribution. Open diamonds used the real-space model. The solid line shows the prediction from Section 2.

redshift space this will transform into:

$$\begin{aligned}
 P(s) &\propto \int_0^\infty r^\alpha \frac{e^{-(s-r)^2/2\sigma_v^2}}{\sqrt{2\pi\sigma_v^2}} \\
 &\propto (\sigma_v)^{\alpha+1} \left[\frac{s}{\sqrt{2}} \Gamma\left(\frac{\alpha+2}{2}\right) {}_1F_1\left(\frac{1-\alpha}{2}, \frac{3}{2}; -\frac{s^2}{2\sigma_v^2}\right) \right. \\
 &\quad \left. + \frac{\sigma_v}{2} \Gamma\left(\frac{\alpha+1}{2}\right) {}_1F_1\left(\frac{-\alpha}{2}, \frac{1}{2}; -\frac{s^2}{2\sigma_v^2}\right) \right], \quad (22)
 \end{aligned}$$

where F is a hypergeometric function.

For a specific case of $\alpha = 2$, Eq. (22) results in:

$$P(s) \propto (\sigma_v^2 + s^2) \left(1 + \text{Erf}\left(\frac{\sigma_v}{\sqrt{2}s}\right) \right) + \sqrt{\frac{2}{\pi}} \sigma_v s e^{-s^2/2\sigma_v^2}, \quad (23)$$

where $\text{Erf}(x)$ is an error function. The distribution of galaxy pairs for $\alpha = 2$ will be:

$$N_{\alpha=2}^{\text{pair}} \propto P(s_1)P(s_2)x_s dx_s d\phi, \quad (24)$$

where $P(s_i)$ is given by Eq. (23) and s_1 and s_2 can be expressed in terms of s and ϕ via Eqs. (11) and (12), after the substitution of x with x_s .

When modelling the theoretical correlation function, Hamilton & Culhane (1996) argue that the difference between $\bar{n}(s)$ and $\bar{n}(r)$ is small. While this is true when creating a model correlation function, it is not true, and we need to use the $\bar{n}(s)$ instead of $\bar{n}(r)$, when we model the data. This is shown in Fig. 2, where we plot $\xi_0(x)$ calculated for $\alpha = 2$ from a mock catalog, assuming that the galaxy distribution follows the one expected from either the real-space or redshift-space calculation. See Section 4 for more details of the calculation.

3.3 Pairs close to the origin

Galaxies that are close to the origin can cause problems as, for such galaxies, the redshift-space displacement can be larger than the distance to the galaxy. This problem is exacerbated because we do not include the velocity of the observer in our calculation. In extreme situations, naively applying the expected redshift-space distortion would place the galaxy on the opposite side of an observer. In order to avoid such problems, we only include galaxy pairs where

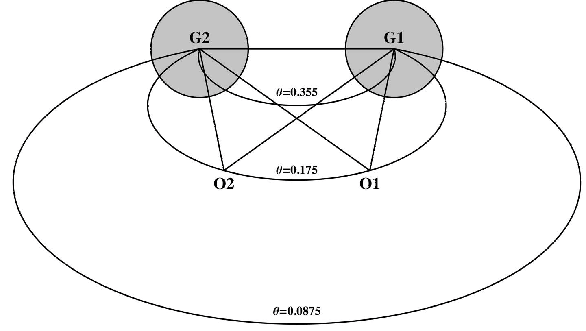


Figure 3. Schematic representation showing the positions at which the origin could be placed for different values of θ . The shaded circles around each galaxy are exclusion zones within which the redshift-space distortions is comparable with the distance to the galaxy. O1 and O2 mark two possible positions for an origin that would give angular galaxy separation of $2\theta = 0.71$.

both galaxies are more than $5\sigma_v$ away from the origin, where σ_v is the 1D velocity dispersion of the galaxy population. For the HV simulation $\sigma_v|_{z=0} = 3.9 h^{-1} \text{ Mpc}$. Fig. 3 shows, for galaxies G_1 and G_2 , the loci of positions at which the origin could be placed for fixed θ . The circles mark the exclusion zones. If one of the galaxies in a pair is inside the exclusion zone in real space, we do not include that pair when we estimate the correlation function. This exclusion is tracked when we calculate the expected galaxy distribution.

3.4 The Hubble Volume Simulation

We apply the procedure outlined in Sec. 3 to analyse wide-angle redshift-space distortions within the Λ CDM Hubble Volume (HV) simulation (Evvard et al. 2002). The Λ CDM HV simulation, covering a $(3000 h^{-1} \text{ Mpc})^3$ box, assumes a cosmological model with $\Omega_m = 0.3$, $\Omega_{CDM} = 0.25$, $\Omega_b = 0.05$, $\Omega_\Lambda = 0.7$, $h = 70$, $\sigma_8 = 0.9$, & $n_s = 1$. We do not apply any galaxy bias, simply Poisson sampling the matter particles to give our “galaxy distribution”; the inclusion of a bias model would not alter the conclusions of this work. We use the periodic nature of the numerical simulation to eliminate boundaries from our pair counts. This means that, by using the above weighting scheme and allowing for the removal of galaxies close to the origin, the expected number of galaxy pairs in the absence of clustering RR can be calculated analytically. We can therefore use the natural estimator $1 + \xi = DD/RR$ (Landy & Szalay 1993), where DD is the measured number of galaxy-galaxy pairs.

4 RESULTS

We have performed 100 runs, each based on a sample of 10^6 galaxies drawn from the $z = 0$ output of the HV Λ CDM simulation. For each unique pair of galaxies within the sample we have selected two locations for the origin, one where the galaxies subject a separation angle of $\theta = 0.355$, chosen to match figure 1 of Papai & Szapudi (2008), and one origin where $\theta = 0.71$, twice this angular separation, to emphasise the wide angle effects on pairs separated by a very wide angle.

We include all pairs with redshift-space separation $x_s < 200 h^{-1} \text{ Mpc}$, and each pair was weighted as described in Section 3.2, based on its real-space separation and angle to the line of sight. Given that, as one can see from Eq. (10), the mode-coupling

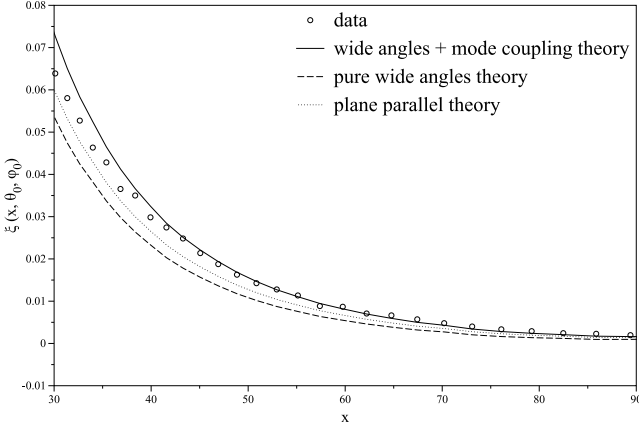


Figure 4. Correlation function as a function of scale for fixed $\theta = 0.355$ and for a bin centered at $\mu = 1.03$, designed to match figure 1 of Papai & Szapudi (2008). The plane-parallel model is shown by the dotted line, the pure wide-angles model by the dashed line and the full mode-coupling prediction with $\alpha = 2$ by the solid line. We expect the match between data and models to be good at scales larger than $40 h^{-1}$ Mpc, because we didn't model the small scale non linearities.

terms depend strongly on the radial galaxy distribution, for both the aperture angles we selected samples with different radial galaxy distributions, in order to test our methodology in different cases; we chose $\alpha = 0, 0.5, 2, 4$:

- $\alpha = 0$ corresponds to the case of a galaxy distribution that has equal density in radial bins of equal width. In this case there are no mode-coupling terms in Eq. (10), so this corresponds to the "pure wide angles" case.
- $\alpha = 0.5$ corresponds to a final real-space distribution of galaxy pair separations with probability density function proportional to $x^2 dx$. This is the same distribution obtained by randomly sampling pairs from the simulation, so the x factor drops out of Eq. (21). Note that, for clarity, we do not present results from this value of α as they are very similar to, and overlap results for $\alpha = 0$. The match between data and theory has the same quality as for the other values of α .
- $\alpha = 2$ matches a distribution of galaxies that are uniformly distributed in volume, so equal volumes contain equal numbers of galaxies. Most planned surveys aim to observe galaxies with this radial distribution. Note that, for this galaxy distribution, the pair distribution goes as $x^5 dx$.
- $\alpha = 4$ represents a steeper radial distribution where more galaxies are found at larger distances. This will increase the effect of the mode-coupling terms in the wide-angle redshift-space distortion formulae (Eq. 21).

We have calculated errors by comparing outputs from 100 subsamples, that cover the same HV volume and so only contain the shot noise element. These errors will therefore underestimate the true error, because they do not fully include the cosmic variance component. However, the HV volume is $(3000 h^{-1} \text{ Mpc})^3$, and we only consider pairs with $x < 200 h^{-1} \text{ Mpc}$, so we expect the shot noise to dominate the error budget. Even so, it is worth pointing out that our primary aim is to consider deviations from plane-parallel theory and that our proposed methodology works to match data with the full mode-coupling theory: the size of the errors is unimportant, provided they are far smaller than the differences between theories.

Fig. 4 shows the correlation function, calculated within a nar-

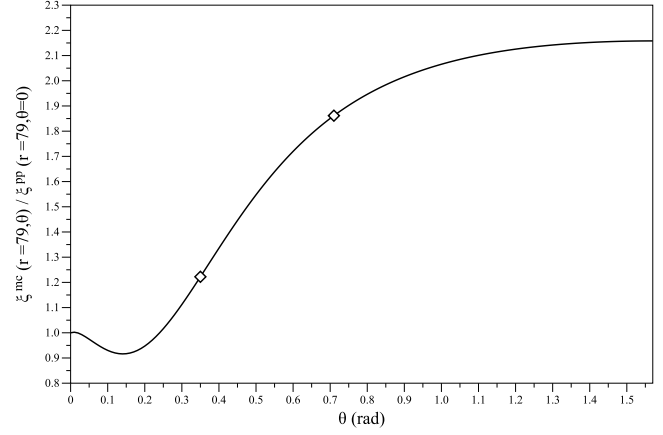


Figure 5. Ratio of theoretical full mode-coupling correlation function to plane-parallel correlation function, computed for $\alpha = 2$ at fixed value of $r = 79 h^{-1}$ Mpc; the points mark the values of θ used in our simulations.

row bin in μ for $\theta = 0.355$ and $\alpha = 2$; this is equivalent to figure 1 of Papai & Szapudi (2008). We are able to fit the theoretical correlation function to the estimate from HV simulations for scales larger than $40 h^{-1}$ Mpc (we do not expect to match perfectly data with theory on smaller scales because we didn't model non-linearities). Looking at plane-parallel, pure wide-angle and full mode-coupling theories, it is clear that only the full mode-coupling theory provides a good fit to the data.

Fig. 5 shows the ratio between the correlation function predicted by the full mode-coupling theory and that for the plane-parallel case, as a function of θ , for a fixed value of $r = 79 h^{-1}$ Mpc, with $\alpha = 2$; from this plot we can see that even for small angles there is a non negligible difference.

In order to analyse RSD, the measured correlation function is usually decomposed into Legendre momenta, which contain all of the RSD signal (Hamilton 1998). Some combination of these momenta is then used to constrain cosmological parameters through their effects on the growth of structure. To see how wide angle effects would modify these measurements we estimate first three even Legendre momenta of the correlation function from HV mock catalog. We measure:

$$\tilde{\xi}_\ell(x) = \frac{\sum_{\mu} DD(x, \mu) L_\ell(\mu)}{\sum_{\mu} RR(x, \mu)}, \quad (25)$$

for $\ell = 0, 2, 4$. Adopting the plane-parallel philosophy (Hamilton 1992), one might be tempted to interpret these functions as:

$$\xi_0^{\text{PP}}(x) = \left(1 + \frac{2}{3}\beta + \frac{1}{5}\beta^2\right) \xi(x), \quad (26)$$

$$\xi_2^{\text{PP}}(x) = -\left(\frac{4}{3}\beta + \frac{4}{7}\beta^2\right) \xi(x), \quad (27)$$

$$\xi_4^{\text{PP}}(x) = \frac{8}{35}\beta^2 \xi(x), \quad (28)$$

where $\xi(x)$ is a real space correlation function and $\beta = f/b$. In fact the functions in Eq. (25) are given by:

$$\tilde{\xi}_\ell(x) = \int W_r(\mu) \xi^s(x, \theta, \mu) L_\ell(\mu) d\mu, \quad (29)$$

where $W_r(\mu)$ is a weight function that appears because of geometrical constraints and because the distribution of μ will not be

uniform. We do not correct for this weight in our measurement from simulations, and apply it to the theoretical calculations that we compare against.

Fig. 6 presents the main results of this work, showing the application of our methodology to sample and analyse data, and comparing against the full mode-coupling predictions. We plot $\xi_0(x)$, $\xi_2(x)$, $\xi_4(x)$ for both the aperture angles and for radial galaxy density distributions corresponding to $\alpha = 0$, $\alpha = 2$ and $\alpha = 4$; as we can see, the contribution of the mode coupling terms increase with α , and as the radial galaxy distribution steepens, more galaxies are moved nearer by the RSD, leading to an increase in the small-scale correlation function. Momenta of the correlation function computed with the full mode coupling theory match remarkably well the data analysed as explained in Sec. 3. We also plot the plane-parallel prediction as a comparison, and this demonstrates how badly this approximation fails for galaxy pairs with wide angular separation. The only parts where our methodology do not match the mode coupling theory are where the correlation multipoles are very small (around 10^{-4}) or for small scales, where non-linearities become important; we also have to take in account that, for the steeper galaxy distributions, we are upweighting results from the same number of pairs as the more shallow galaxy distributions so, although the signal is stronger, the relative error will be the same.

5 DISCUSSION AND CONCLUSIONS

Redshift-Space Distortion Analyses are a powerful tool for cosmology, but incoming data need to be analysed very carefully in order to fully extract all available information. Until now RSD analyses have concentrated on using the plane-parallel approximation (with a few exceptions including Okumura et al. 2008; Pope et al. 2004; Matsubara 2004); this is almost correct if the survey is narrow, but when galaxy surveys with wide field of view data will be available, there will be a consistent number of galaxy pairs separated by wide angles and in this case the plane-parallel approximation fails.

This approximation arises from not taking in account some of the terms in the Jacobian relating redshift- to real-space; in this paper we considered its exact expression, and this causes additional, non-diagonal terms in the correlation function. We then use the expansion of the correlation function in a base of tripolar spherical harmonics, as suggested in Papai & Szapudi 2008; following the formalism developed in Szapudi 2004; Papai & Szapudi 2008, we make predictions for the momenta of the correlation function for galaxy pairs at fixed angular separation, and we test them against data from the Hubble Volume Simulation.

In order to do this we have had to introduce a new methodology: rather than creating a single sample of galaxies in redshift-space from which we can count pairs, we have instead dynamically applied RSD on a pair-by-pair basis, choosing an origin for each. By including weighting functions in x and μ we can match results from the more traditional approach. This allows us to only consider galaxy pairs at particular values of θ .

To show both the correctness of our methodology and the deviation from the plane-parallel situation we tested galaxies separated by two different fixed values of θ ; the mode coupling terms are also strongly dependent on the galaxy radial distribution, so we have tested simulations with 4 different number density distributions, for both values of θ .

We show that taking in account the wide angle and mode coupling terms (that are of the same order, as stated in Papai & Szapudi 2008) give a clear deviation from the plane-parallel theory; using

the exact theory and our methodology, we can match the results of simulations, the agreement between data and theory being remarkable, especially considering how crude our modelling of the HV correlation function is (we use a measurement of the 3D real-space correlation function as our baseline model, and we do not include a correction for fingers-of-god type effects). For RSD measurements made within radial bins, it will be vital to match the theory to the exact distribution of galaxies observed.

In a measurement of RSD from real data, the final result will be a weighted average over different opening angles, to take account for the fraction of galaxy pairs separated by a θ angle, so in wide surveys one has to discard the plane-parallel approximation, or face losing a considerable amount of information. For this reason our methodology will be particularly useful for incoming and future redshift Surveys, such as the Baryon Oscillation Spectroscopic Survey (BOSS; Schlegel et al. 2009a), BigBOSS (Schlegel et al. 2009b), and Euclid (Laureijs et al. 2009); the importance of this methodology for current and future experiments will be considered in a subsequent paper (Samushia et al. in preparation).

6 ACKNOWLEDGEMENTS

AR is grateful for the support from a UK Science and Technology Facilities Research Council (STFC) PhD studentship. WJP is grateful for support from the European Research Council and from the Leverhulme Trust and STFC. LS acknowledges support from European Research Council, Georgian National Science Foundation grant ST08/4-442 and SNSF (SCOPES grant No 128040). AR would like to thank G. W. Pettinari for the useful discussions. Simulated data was calculated and analysed using the COSMOS Altix 3700 supercomputer, a UK-CCC facility supported by HEFCE and STFC in cooperation with CGI/Intel.

REFERENCES

- Ballinger W. E., Peacock J. E., Heavens A. F., 1996, MNRAS, 282, 877
- Blake C., et al., 2010, MNRAS accepted, [arXiv:1003.5721]
- Cabre A., Gaztanaga E., 2009, MNRAS, 396, 1119
- Cole S., et al., 2005, MNRAS, 362, 505
- Colless M., et al., 2003, astro-ph/0306581
- Eisenstein D.J., et al., 2005, ApJ, 633, 560
- Evrard A.E., et al., 2002 ApJ, 573, 7
- Efstathiou G., Sutherland W.J., Maddox S.J., 1990, Nature, 348, 705
- Fisher K.B., Scharf C.A., Lahav O., 1994, MNRAS, 266, 219
- Frieman J., Turner M., Huterer D., 2008, Ann. Rev. Astron. Astrophys., 46, 385
- Gaztanaga E., Cabre A., Hui L., 2008, [arXiv:0807.3551]
- Guzzo, L., 2009, Nature, 541, 2008
- Hamilton A.J.S., 1992, ApJ, 385, L5
- Hamilton A.J.S., Culhane M., 1996, MNRAS 278, 73
- Hamilton A.J.S., “Linear redshift distortions: A review”, in “The Evolving Universe”, ed. D. Hamilton, pp. 185-275 (Kluwer Academic, 1998) [astro-ph/9708102]
- Hawkins E. et al., 2003, MNRAS, 346, 78
- Heavens A.F., Taylor A.N., 1995, MNRAS, 275, 483
- Kaiser N., 1987, MNRAS, 227, 1
- Kessler R., et al., 2009, ApJS, 185, 32
- Landy S. D., Szalay A. S., 1993, ApJ, 412, 64

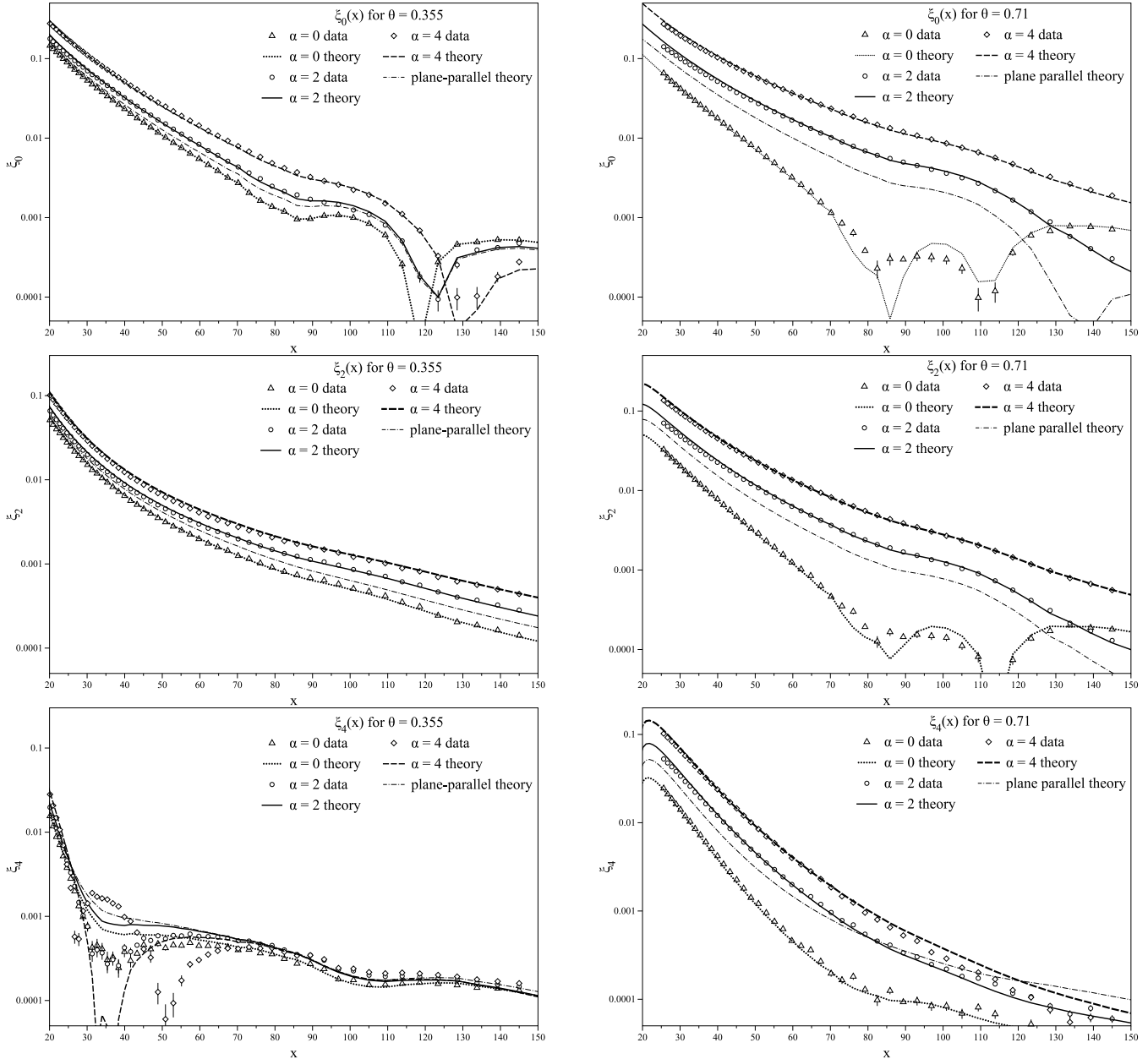


Figure 6. $\xi_0(x)$, $\xi_2(x)$, $\xi_4(x)$ for angular galaxy pair separations of $\theta = 0.355$ (left column) and $\theta = 0.71$ (right column) for different power law radial galaxy density distributions; lines are the expected values from the theory of Papai & Szapudi (2008) with wide angle and mode-coupling effects, with $\alpha = 0$ (dotted), $\alpha = 2$ (solid), and $\alpha = 4$ (dashed); dot-dashed lines are plane parallel predictions. Symbols were measured from the HV mocks, with $\alpha = 0$ (triangles), $\alpha = 2$ (circles), and $\alpha = 4$ (diamonds).

Laureijs R., et al., 2009, “Euclid Assessment Study Report for the ESA Cosmic Visions”
 Matsubara T., 2004, *ApJ*, 615, 573
 Okumura T., Matsubara T., Eisenstein D.J., Kayo I., Hikage C., Szalay A.S., Schneider D.P., 2008, *ApJ*, 676, 889
 Papai P., Szapudi I., 2008, *MNRAS*, 389, 292
 Peacock J.A., et al., 2001, *Nature*, 410, 169
 Percival W.J., et al., 2001, *MNRAS*, 327, 1297
 Percival W.J., et al., 2004, *MNRAS*, 353, 1201
 Percival W.J., et al., 2007a, *ApJ*, 657, 645
 Percival W.J., Cole S., Eisenstein D., Nichol R., Peacock J.A., Pope A., Szalay A., 2007b, *MNRAS*, 381, 1053
 Percival W.J., White M., 2009, *MNRAS*, 393, 297

Percival W.J., et al., 2010, *MNRAS*, 401, 2148
 Perlmutter S., et al., 1999, *ApJ*, 517, 565
 Pope A.C., et al., 2004, *ApJ*, 607, 655
 Riess A.G., et al., 1998, *AJ*, 116, 1009
 Samushia L., Raccanelli A., Percival W.J., in preparation
 Sanchez A.G., Crocce M., Cabre A., Baugh C.M., Gaztanaga E., 2009, *MNRAS*, 400, 1643
 Schlegel D., White M., Eisenstein D.J., 2009a, [arXiv:0902.4680]
 Schlegel D., et al., 2009b, [arXiv:0904.0468]
 Simpson, F., Peacock, J. A., 2009, [arXiv:0910.3834]
 Szalay A.S., Matsubara T., Landy S.D., 1998, *ApJ*, 498, L1
 Szapudi I., 2004, *PhRvD*, 70, 083536
 Varsholovich D. A., Moskalev A. N., & Khershonski V. K., 1988,

Quantum Theory of Angular Momentum (Singapore: World Scientific)

York, D.G., et al., 2000, AJ, 120, 1579

Zehavi, I., et al., 2005, ApJ, 630, 1